Decadal Changes in the Mode Waters in the Midlatitude North Pacific

TAMAKI YASUDA AND KIMIO HANAWA

Department of Geophysics, Graduate School of Science, Tohoku University, Sendai, Japan

(Manuscript received 14 June 1995, in final form 5 August 1996)

ABSTRACT

Temporal changes in the properties of the North Pacific subtropical mode water (NPSTMW) and the North Pacific central mode water (NPCMW), which occurred around the mid-1970s, are investigated using temperature data composited for the two decades bounded by the mid-1970s: 1966–75 and 1976–85. Properties of these mode waters changed greatly after the mid-1970s. The colder NPCMW was formed and widely distributed during 1976–85. In the NPSTMW formation area, warmer water occupied the southwestern part, and colder water occupied the northeastern part during 1976–85. The cause of this change is discussed with regard to the heat flux and wind stress data. The cooling can be explained as a result of changes in surface heat flux and heat divergence in the Ekman layer, that is, a larger amount of heat released from the ocean surface and an increased southward Ekman transport of cold water due to intensification of the westerlies. In particular, the latter plays a dominant role in the observed cooling. On the other hand, the warming in the southwestern part of the NPSTMW area cannot be explained by the above mechanism alone. Time series of the Sverdrup transport, the Kuroshio transport, and the thermal structure of the upper ocean reveal that the subtropical gyre intensified after the mid-1970s, suggesting that increased advection of warm water by the Kuroshio from lower latitudes to the south of Japan contributed to the observed warming.

1. Introduction

The climate change that occurred in the North Pacific during the mid-1970s has been shown to reveal decadal variability of the atmosphere–ocean coupled system. Among its various aspects, the decadal variability of the ocean has been investigated mainly using sea surface temperature (SST; Davis 1976; Nitta and Yamada 1989; Wallace et al. 1990; Tanimoto et al. 1993). For example, Tanimoto et al. (1993) investigated the multiple timescale variability of SST in the North Pacific from 1950 to 1986. In their analysis of empirical orthogonal functions (EOFs) for the decadal timescale, some quasi-steady periods and some rapid transitions were recognized. One of these quick transitions was seen in the mid-1970s. This transition has a strong connection with the variation of the atmospheric circulation characterized by the Pacific–North American (PNA) teleconnection pattern related to the intensification of the Aleutian low (Trenberth 1990; Wallace et al. 1990; Trenberth and Hurrel 1994). As far as the mechanism of SST variability, Cayan (1992b,c) studied large-scale variations of the heat flux and showed that it is closely related to the PNA pattern and the monthly SST tendency. Model studies have also contributed to understanding the mechanism of SST variability. Using an atmosphere–ocean coupled model, Tokioka et al. (1992) showed that strengthening of the Ekman transport caused a decrease in SST in the central North Pacific. Miller et al. (1994) found that two quasi-steady states of the upper ocean before and after the mid-1970s were mainly maintained by a difference in vertical mixing in the mixed layer. Strong vertical mixing after the mid-1970s effectively lowered the temperature in the subsurface layers (Haney 1980, 1985).

The change in the ocean interior structure around the mid-1970s was described by Watanabe and Mizuno (1994). They showed that the upper layer of the central North Pacific became colder after 1975 and that the influence of its anomalous cooling proceeded southward with time. They speculated that its spread was caused by the ventilation process in the thermocline.

The upper-ocean thermal structure of the midlatitude North Pacific is largely characterized by the two major mode waters: One is the North Pacific subtropical mode water (NPSTMW) and the other is the North Pacific central mode water (NPCMW). Since they reflect atmosphere–ocean interaction, they are good indicators of the temporal variability of the upper-ocean thermal structure.

The NPSTMW is distributed in the northwestern part of the subtropical gyre and is characterized by a thermostad of 15°–19°C (e.g., Masuzawa 1969; Hanawa and Suga 1995). The process of formation and distribution of NPSTMW has been considered as follows: NPSTMW

Corresponding author address: Dr. Tamaki Yasuda, Physical Oceanography Laboratory, Department of Geophysics, Tohoku University, Aoba-ku, Sendai 980-77, Japan.

is formed immediately south of the Kuroshio Extension in winter due to a huge amount of heat released from the ocean to the atmosphere and is spread widely throughout the northwestern subtropical gyre by the Kuroshio recirculation system (e.g., Masuzawa 1969, 1972; Hanawa 1987; Suga et al. 1989; Suga and Hanawa 1990, 1995b; Bingham 1992).

Temporal variations in the spatial extent and properties of the NPSTMW are closely related to the wintertime heat flux in the formation area (e.g., Suga and Hanawa 1995a). Bingham et al. (1992) compared the thermal structure over the northwestern part of the North Pacific subtropical gyre between two pentads of 1938–42 and 1978–82. NPSTMW was thicker and more confined geographically in the western part during 1938–42. They attributed the thicker NPSTMW to the stronger cooling in winter during 1938–42, which was deduced by the intensity of the East Asian wintertime monsoon and other indices. On the other hand, they inferred that the more confined distribution resulted from reduced advection by the Kuroshio current system because of the spindown of the gyre suggested from the thermal structure during 1938–42. Their argument implies that NPSTMW properties, at least its spatial distribution, can also vary with ocean circulation through the spinup or spindown of the subtropical gyre.

The NPCMW was first discussed by Nakamura (1996) and Suga et al. (1997). NPCMW is distributed mainly at 30°–40°N and 170°E–150°W as a 9°–13°C thermostad (Suga et al. 1997). Nakamura (1996) described the climatological features of NPCMW based on the Levitus (1982) temperature and salinity data. He showed low potential vorticity water centered at approximately 26.25 σ_θ spreading in the central North Pacific. Furthermore, Nakamura (1996) and Suga et al. (1997) examined the distribution of the wintertime mixed layer and concluded that NPCMW was formed by wintertime deep convection north of its distribution area. Since atmosphere–ocean interaction affects wintertime convection, this interaction may play a great role in causing the NPCMW variations. Temporal variability of the NPCMW, however, has not been examined yet.

In this study, we describe the changes in the two mode waters, the NPSTMW and the NPCMW, that occurred around the mid-1970s. Since those waters characterize the upper thermal structure in the midlatitude North Pacific, understanding of the changes in those waters leads to an understanding of the change in the upper-ocean thermal structure in the midlatitude North Pacific. We discuss the cause of changes in mode waters in terms of wind stress and heat flux. We also examine the influence of ocean currents, that is, the Ekman and geostrophic flows, on the properties of the mode waters.

The contents of this paper are as follows: Section 2 describes the temperature, wind stress, SST, and heat flux data used in this study. In section 3, the two decades used in the composite analysis are determined and the decadal changes in the properties of the NPSTMW and the NPCMW are discussed. The causes of those changes in mode waters are discussed along with the atmospheric and oceanic factors in section 4. Section 5 contains concluding remarks.

2. Data and methods

a. Temperature data

Temperature data were selected from the dataset released by the National Oceanographic Data Center (1991). This dataset includes oceanographic station (SD2), salinity/conductivity–temperature–depth (S/CTD), expendable bathythermograph (XBT), mechanical bathythermograph (MBT), selected level bathythermograph (SBT), and IGOSS radio message bathythermograph (IBT) data. The number of the observation is considerably reduced before the mid-1960s. Thus, in the present study, the analysis is carried out for 10°–50°N, 120°E–100°W during the period 1966–85. The distribution of all stations used is shown in Fig. 1.

Since most of these data are confined to 460 m and shallower, we only considered data above 460 m. XBT fall rate error (Hanawa et al. 1995) was corrected; the measured depth profile was corrected by using the equation $Z_c = 1.034 \times Z_m$, where Z_c is the corrected depth profile and Z_m is the measured one. The corrected data were linearly interpolated to regular 20-m depth intervals. For each year, 2° × 2° (latitude × longitude) seasonal averages were made at each depth using a Gaussian filter with an *e*-folding scale of 0.5° in latitude and 0.75° in longitude. Winter was defined as the months January–March, spring as April–June, summer as July–September, and fall as October–December.

In compositing data we first formed a seasonal mean for each year and then averaged the seasonal means for each decade. This reduces the seasonal and year-to-year biases in the distribution of observations. Since dynamical disturbances of mesoscale eddies inevitably exist within our study data, and are important in the variability of the upper thermal structure, we are not able to show that there are significant temperature differences between the two decades. However, we will show that the temperature differences make sense in terms of the heat flux, the Ekman heat transport, and the geostrophic transport in section 4. Thus, we believe that the temperature differences shown in this study are plausible.

b. SST, wind, and heat flux data

In order to discuss the causes for the decadal changes in the mode waters, we use SST, wind stress, and heat flux data. These data were computed by Tanimoto et al. (1997) from Comprehensive Ocean Atmosphere Data Set (COADS) marine reports. This dataset includes monthly 5° × 5° data from 1950 to 1990. The procedures of the calculation are described in Tanimoto et al. (1993) for SST and Tanimoto et al. (1997) for wind stress and

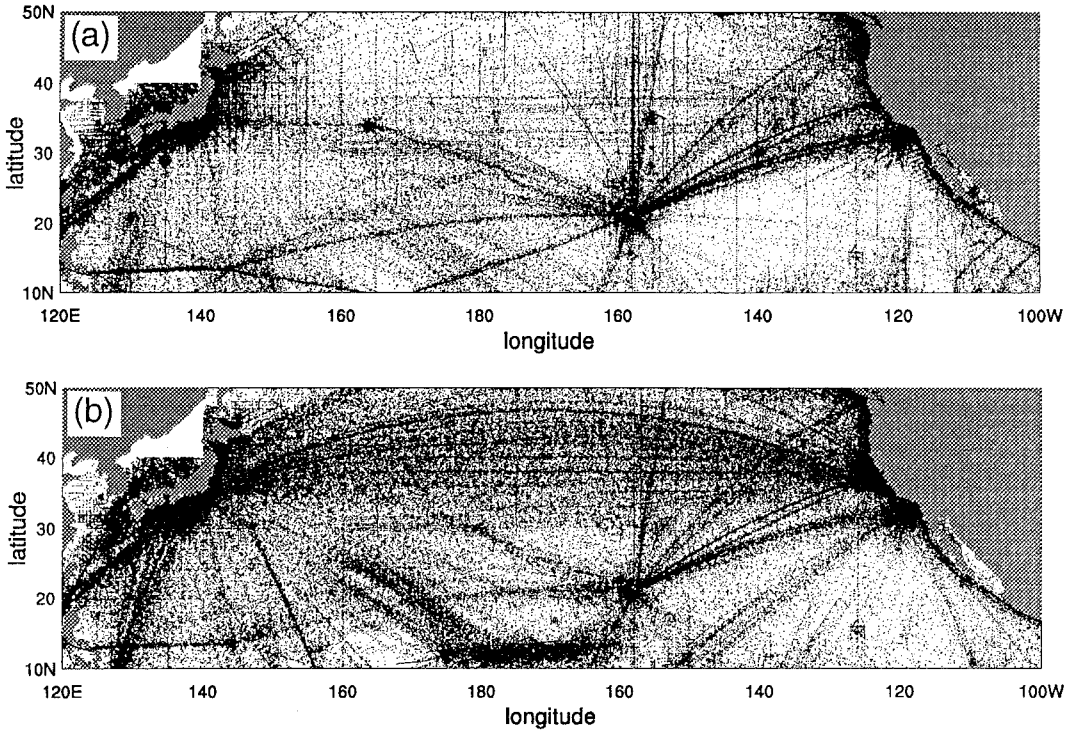

FIG. 1. Distribution of stations used in the present study for (a) 1966–75 and (b) 1976–85. The numbers of the stations are 247882 and 308098 for 1966–75 and 1976–85, respectively.

heat flux. In this study, seasonal data for each year and annual mean data are calculated from the original monthly data in Tanimoto et al. (1997). Seasons for wind stress and heat flux were different from those of temperature data. Winter was defined from December to February, etc.

Sources of error in calculating heat flux were discussed by Weare (1989) and Cayan (1992a–c). Random errors can be reduced by averaging several observations. Since we examine seasonal and 10-yr mean heat fluxes in this study, those errors are considerably reduced. Time invariant bias can be estimated mainly by considering the difference between the two decades in this study. There are also time variant biases. Many authors remove linear trends considered to be partly caused by changes in instrumental practices. However, we do not know to what extent those changes affect the trends. Hanawa et al. (1996) examined whether the change in the wind field over the North Pacific during the mid-1970s is real or an artifact of changing instrumentation such as the change in the heights of ship anemometers. They compared the wind stress fields with sea level pressure and the resulting geostrophic wind fields, and concluded that instrumental effects were small. Hence, we do not remove a linear trend from the original data. Furthermore, since heat flux results show spatially systematic features and are consistent with other results (e.g., Cayan 1992b), we believe that our results are not problematic.

3. Decadal changes in the NPSTMW and the NPCMW

In this section, we describe how the temperature and distribution of the NPSTMW and the NPCMW changed after the mid-1970s. Watanabe and Mizuno (1994) showed that SST anomalies averaged from 35° to 45°N became negative in and after 1976. Decadal variations of SST studied in Tanimoto et al. (1993) indicate that a warm phase of the decadal SST pattern changed to a cold one in 1976 and continued until 1985. The period 1966–75 is generally warmer, although there were periods before 1970 when SST anomalies were near zero. We thus chose the two decades 1966–75 and 1976–85, for compositing the temperature data. Also, since it is known that variability at interannual timescales is large in the northwestern part of the North Pacific subtropical gyre (Suga and Hanawa 1995a), we chose these above periods in order to prevent variability at the interannual timescales from appearing in the composited data. We then present results based on the composited analysis of changes in the NPSTMW and the NPCMW. In compositing data, a spatial Hanning filter with weight function of 0.25, 0.5, and 0.25 is operated three times zonally and once meridionally.

The two mode waters are formed by deep convection due to surface cooling in winter. In climatology, a deep wintertime mixed layer is formed mainly in the area of 28°–35°N, 140°–160°E and north of 38°N in the

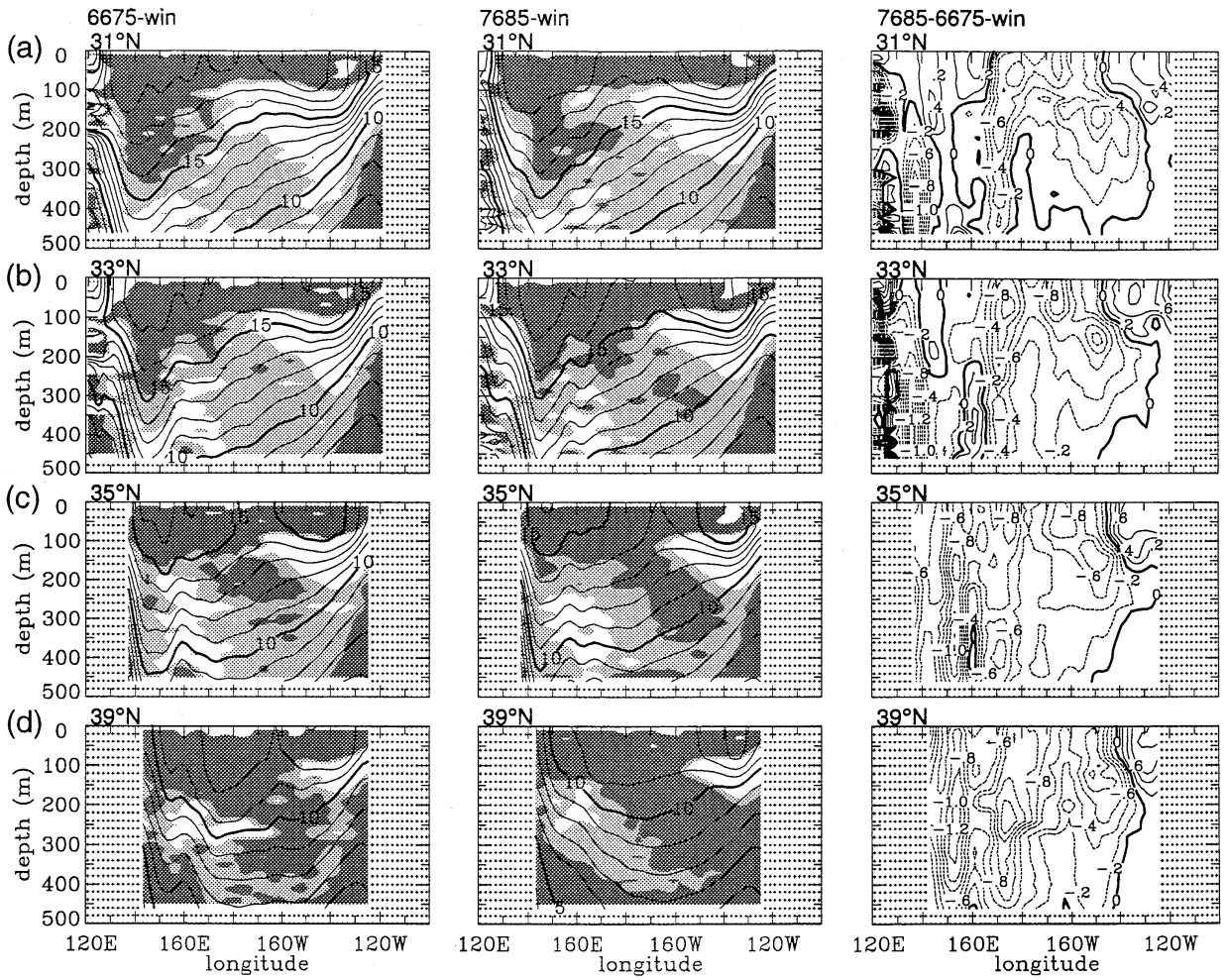

FIG. 2. Zonal temperature sections in winter for 1966–75, 1976–85, and the difference between these two decades at (a) 31°N, (b) 33°N, (c) 35°N, and (d) 39°N. Contour intervals are 1.0°C for 1966–75 and 1976–85, and 0.2°C for the difference. Dashed contours denote negative differences. Areas with the vertical temperature gradients less than 2.0°C/100 m are hatched lightly and those with gradient less than 1.5°C/100 m are hatched darkly.

central North Pacific. The former corresponds to the formation area of NPSTMW and the latter corresponds to that of the NPCMW (Suga and Hanawa 1990; Huang and Qiu 1994; Nakamura 1996). First, we compare the wintertime thermal structures in those areas. Figure 2 shows temperature sections along 31°, 33°, 35°, and 39°N in winter composited for the two decades. Thermostads are highlighted by hatching the layers of vertical temperature gradient less than 2.0°C/100 m lightly and those less than 1.5°C/100 m darkly. Figure 2 also presents the temperature difference between the two decades. In Figs. 2a–c, the thermal structure that represents the southward Sverdrup flow and the northward Kuroshio is recognized. Furthermore, the surface mixed layer is fairly deep in the area centered at 150°E and its temperature ranges around 15°–19°C. These areas correspond to the NPSTMW formation area. In the figures of temperature difference, there are positive areas east of 145°W and negative areas between 170°E and 145°W at all latitudes. On the other hand, the temperature difference west of 170°E varies with latitude; that is, a positive area is recognized in the 31°N section, but is no longer apparent at 35°N. These show that the NPSTMW formed during 1976–85 is warmer than that formed during 1966–75 in the southwestern part of its formation area, but colder in the northeastern part. Figure 2d shows the temperature section that corresponds to a part of the NPCMW formation area. A deep mixed layer develops at around 180° and the temperature difference reaches −1.0°C in that area. Therefore, colder NPCMW was formed during 1976–85. The above results are consistent with earlier results regarding the SST change that occurred in the mid-1970s (Wallace et al. 1990; Tanimoto et al. 1993; Trenberth and Hurrel 1994; Watanabe and Mizuno 1994; Deser and Blackmon 1995).

In spring, NPSTMW subducts under the seasonal thermocline and is advected widely in the northwestern

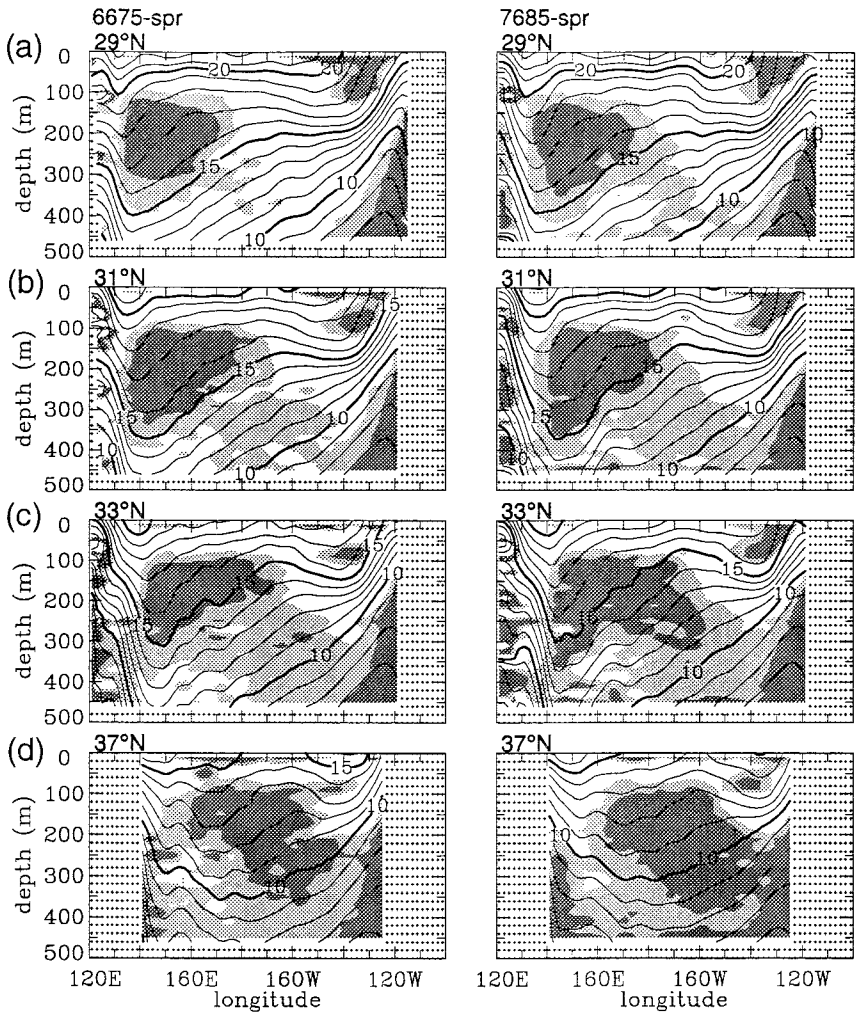

FIG. 3. Zonal temperature sections in spring for 1966–75 and 1976–85 at (a) 29°, (b) 31°, (c) 33°, and (d) 37°N. Contour intervals are 1.0°C. Areas with vertical temperature gradient less than 2.0°C/100 m are hatched lightly and those with gradient less than 1.5°C/100 m are hatched darkly.

part of the subtropical gyre with characteristics of the thermostad formed in winter. In this study, NPSTMW is defined as the thermostad in which the vertical temperature gradient is less than 1.5°C/100 m. It is shown in Figs. 2 and 3 by the dark hatching. Temperature sections along 29°, 31°, and 33°N in spring are shown in Figs. 3a–c. From the temperature at the lower boundary of the NPSTMW thermostad, it is apparent that colder NPSTMW exists for 1976–85 than for 1966–75. Also, the NPSTMW thermostad for 1976–85 is in continuous contact with the 11°–13°C thermostad corresponding to a part of the NPCMW. This colder NPSTMW is probably formed east of 160°E at higher latitudes such as 35°N in winter (Fig. 2c). Figure 3d shows the temperature section along 37°N. The temperature of the NPCMW thermostad with vertical gradient less than 1.5°C/100 m exhibits considerable difference between the two decades: 9°–14°C for 1966–75 and 8°–13°C for 1976–85.

We can also see a change in the mode waters, during the summer. Figure 4 shows scatterplot diagrams for the summer temperature and its vertical gradient at 20°–40°N, 130°E–130°W. Since the minimum of the vertical temperature gradient represents the vertical core of the mode water, that minimum is a good indicator of the properties of the mode water (Suga et al. 1997). In Fig. 4, there are minima of the vertical temperature gradient at 16°–17°C and 10°–11°C, corresponding to the NPSTMW core and the NPCMW core. In both the NPSTMW and the NPCMW, the core temperature of the mode water is clearly different between the two decades.

In order to highlight the spatial changes in the mode waters between the two decades, horizontal maps of these core temperatures are drawn in Fig. 5. The NPSTMW core is colder during 1976–85 in most of the NPSTMW area (Fig. 5a). NPSTMW during 1966–75 is warmer than 16.5°C at 140°–160°E, whereas the 1976–

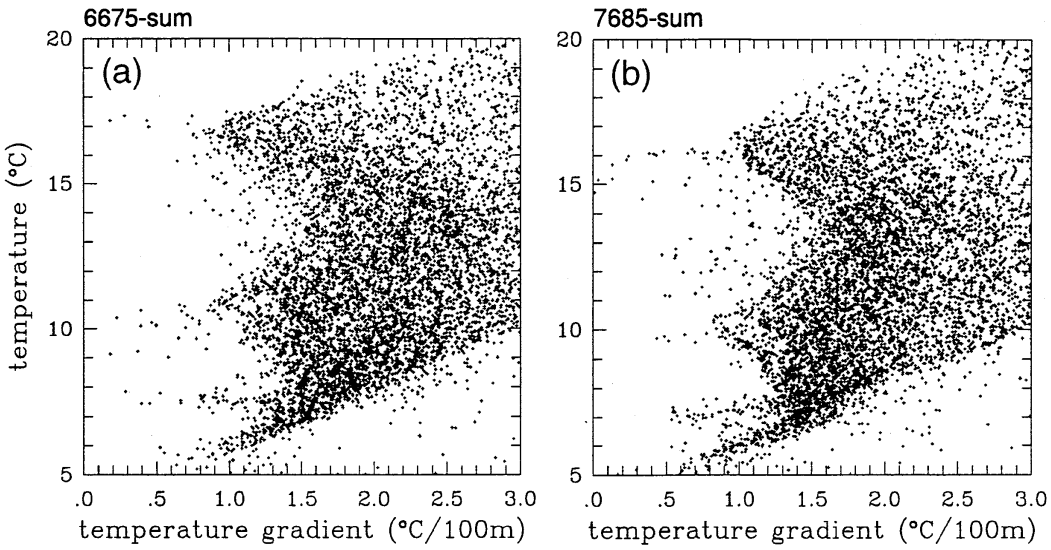

FIG. 4. Scatterplots of temperature versus temperature gradient for summer temperature profiles in the area 20°–40°N and 130°E–130°W for (a) 1966–75 and (b) 1976–85.

85 field indicates the temperature below 16.5°C in most of the NPSTMW area. On the other hand, warmer NPSTMW is seen west of 140°E during 1976–85. This warmer NPSTMW corresponds to water formed west of 160°E in winter (Fig. 2a). Furthermore, NPSTMW spreads farther to the east of 170°E during 1976–85. This suggests that intensified eastward currents corresponding to the spinup of the gyre cause more eastward advection of NPSTMW. In the NPCMW core, we can see southward shifts of temperature contours and a larger area of 9°–11°C contours for 1976–85 than 1966–75 (Fig. 5b). This represents an increase in volume of colder NPCMW.

4. Mechanisms of the oceanic decadal changes

a. Heat flux

On the interannual timescale, the properties of the NPSTMW vary with the strength of the cold-air surge of the East Asian wintertime monsoon. In earlier studies of NPSTMW variability, it has been shown that there is a large amount of heat released through the surface over the NPSTMW formation area during the wintertime monsoon. The relationship of surface heat flux with the properties of NPSTMW has been discussed (e.g., Suga and Hanawa 1995a). In this study, we examine the causes of the decadal change in the properties of the

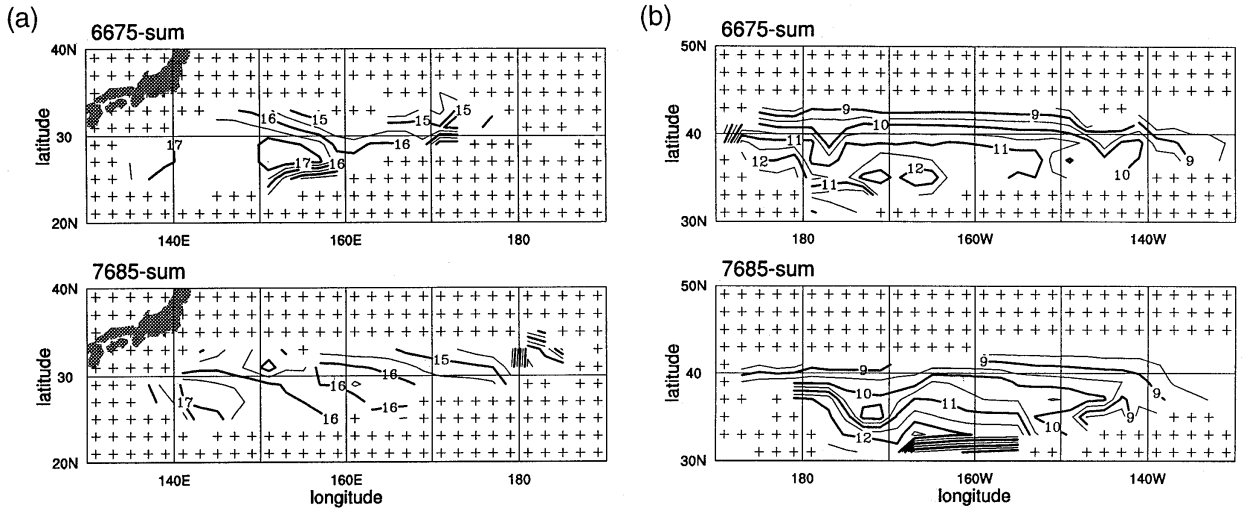

FIG. 5. Temperature distributions on the surface of vertical temperature gradient minimum corresponding to (a) NPSTMW and (b) NPCMW. The contour intervals are 0.5°C. For areas where the vertical temperature gradient is greater than 2.0°C/100 m, contours are not displayed.

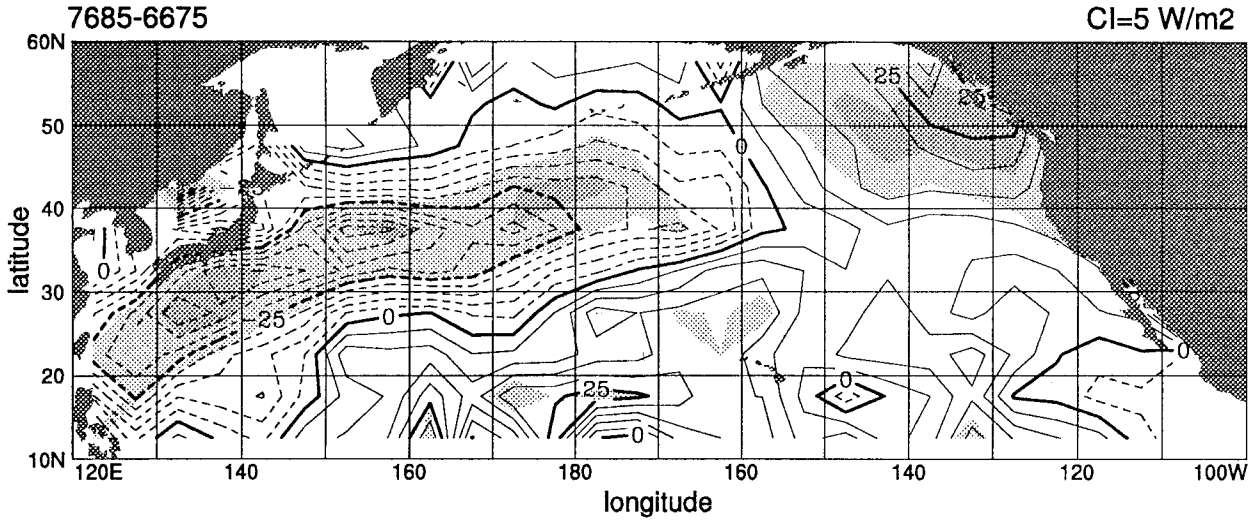

FIG. 6. Difference of the wintertime net heat flux fields between the two decades. Contour intervals are 5 W m^{-2} and dashed contours denote a larger heat release during 1976–85 than 1966–75. Areas with confidence greater than 90% are hatched lightly and those with confidence greater than 99% darkly.

NPSTMW and the NPCMW. Figure 6 shows the difference of wintertime net heat flux through the sea surface between 1966–75 and 1976–85. It indicates a larger area of the western North Pacific where the heat loss during 1976–85 is more more than 25 W m^{-2} greater than the earlier decade. This area is consistent with that of a larger amount of heat release connected with the strong Aleutian low due to the active PNA pattern (Cayan 1992b). The Aleutian low became stronger after the mid 1970s (Trenberth and Hurrel 1994; Hanawa et al. 1996) as seen in the maps of wind stress vectors (Fig. 7). Therefore, the feature shown in Fig. 6 is related to the PNA pattern. Since that area also corresponds to formation areas of NPSTMW and NPCMW, decadal changes in the heat flux must have as great an influence on the mode waters as interannual changes. However, we have to examine how the difference of heat release alone can explain the changes in the temperature shown in Fig. 2.

b. Heat divergence in the Ekman layer

As a result of the intensification of the westerlies centered by the Aleutian low, the strength of the surface Ekman flow changes and consequently so does the heat transport in the Ekman layer (Deser and Blackmon 1995). These changes consequently influence the temperature in the upper ocean. Assuming that the temperature in the Ekman layer is identical to SST, the heat transport in that layer, $\vec{H}_E$, is calculated in terms of the wind stress ($\boldsymbol{\tau}$) and SST (T_S) averaged from December to February,

$$\vec{H}_E = C_w \frac{\mathbf{k} \times \boldsymbol{\tau}}{f} T_S,$$

where $C_w = 4.0 \times 10^3$ J K^{-1} kg^{-1} is the specific heat of sea water, f is the Coriolis parameter, and $\mathbf{k}$ is a unit vertical vector. Changes in divergence of that transport, $\boldsymbol{\nabla} \cdot \vec{H}_E$, can contribute to changes in the heat content as changes in the surface can. The difference of that divergence between the two decades is shown in Fig. 8. Because of the intensification of the westerlies, a greater amount of heat is lost north of 30°N during 1976–85 than during 1966–75, and it exceeds 50 W m^{-2} along 38°N in the central North Pacific. Heat loss in the Ekman layer is dominant in the central North Pacific, whereas in the western North Pacific, the change in surface heat flux is larger than that of the Ekman heat divergence.

Figure 9 shows the sum of the difference of the heat flux through the sea surface (Fig. 6) and the difference of the Ekman heat divergence (Fig. 8). A negative net change appears along the western boundary and throughout most of the area north of 30°N. We will now estimate how much of the temperature difference between the two decades can be explained from the difference of the heat loss shown in Fig. 9. If the typical mixed layer depth D is assumed to be constant 200 m, the resulting temperature difference ΔT between the two decades is given by

$$\Delta T = \frac{\Delta Q}{C_w \rho D},$$

where ΔQ is the difference of the heat loss shown in Fig. 9 multiplied by 3 months and $\rho = 1025$ kg m^{-3} is the density of sea water. With these parameters, 100 W m^{-2} of heat loss corresponds to 0.95°C of temperature reduction.

In the central North Pacific area (40°N, 180°), since the heat loss change is about 70 W m^{-2}, the temperature reduction is estimated as about 0.7°C. On the other hand, it is about 0.3°C in the Kuroshio area (30°N, 140°E) as

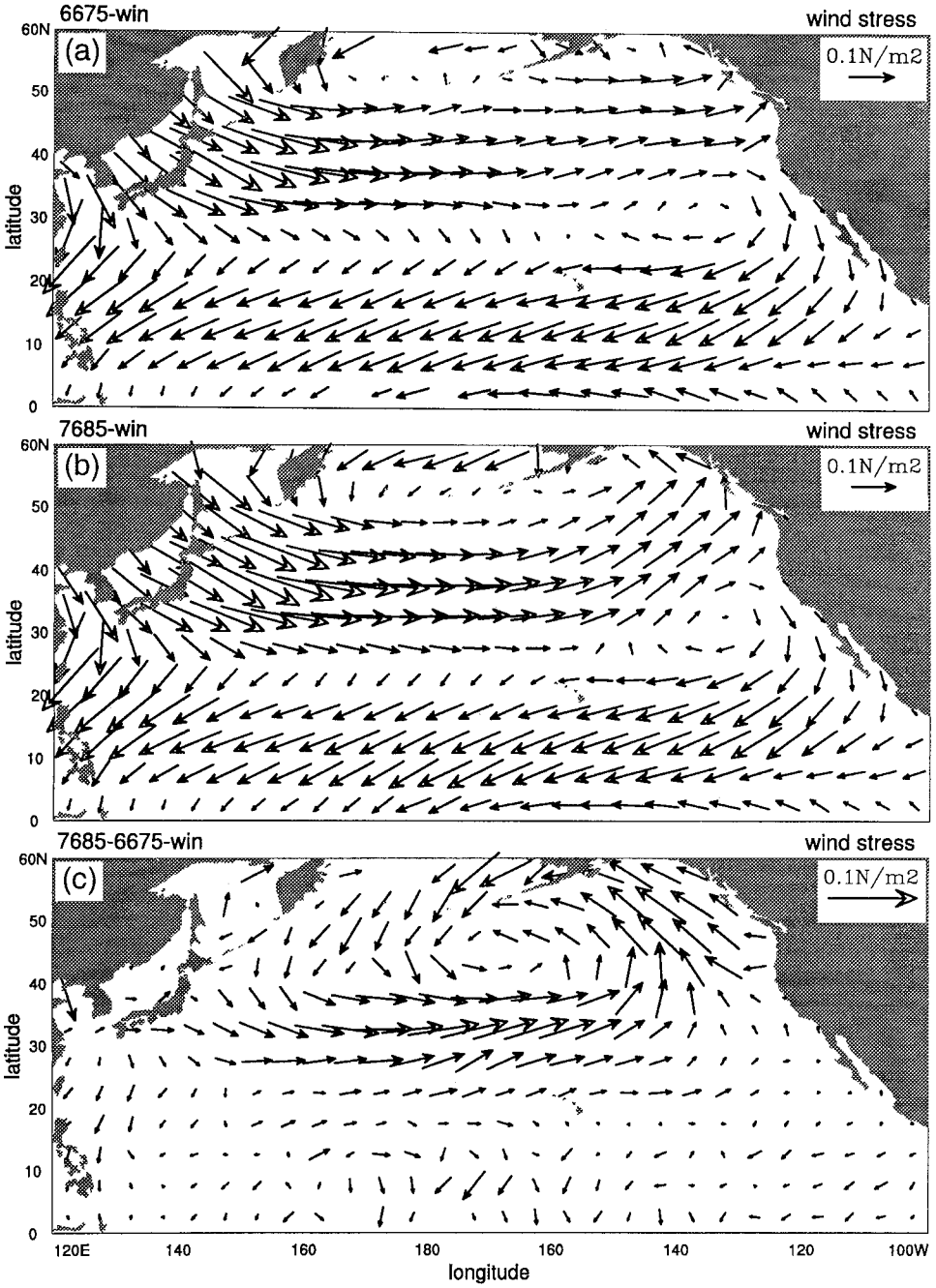

FIG. 7. Difference of the wintertime wind stress fields between 1966–75 and 1976–85.

a result of 30 W m^{-2} of heat loss change. Since the former value is comparable to the observed temperature difference (Fig. 2d), we consider that a change in the Ekman heat divergence is the major cause for the lower temperature during 1976–85 in the central North Pacific as suggested by Deser and Blackmon (1995). Haney (1980) and Miller et al. (1994) showed that vertical mixing was the most important process for changing the temperature in the subsurface layer, even with a large Ekman transport. In the above discussion, the process of mixed layer deepening is ignored. However, since the importance of Ekman transport for cooling in the central North Pacific is also consistent with the results of model studies by Tokioka et al. (1992), we believe that heat loss via Ekman heat divergence is the main cause of the mixed layer deepening through vertical mixing, which must redistribute colder SST anomalies.

The estimated heat loss suggests a 0.3°C decrease of the surface layer temperature in the Kuroshio area. The observed difference in temperature, however, is positive

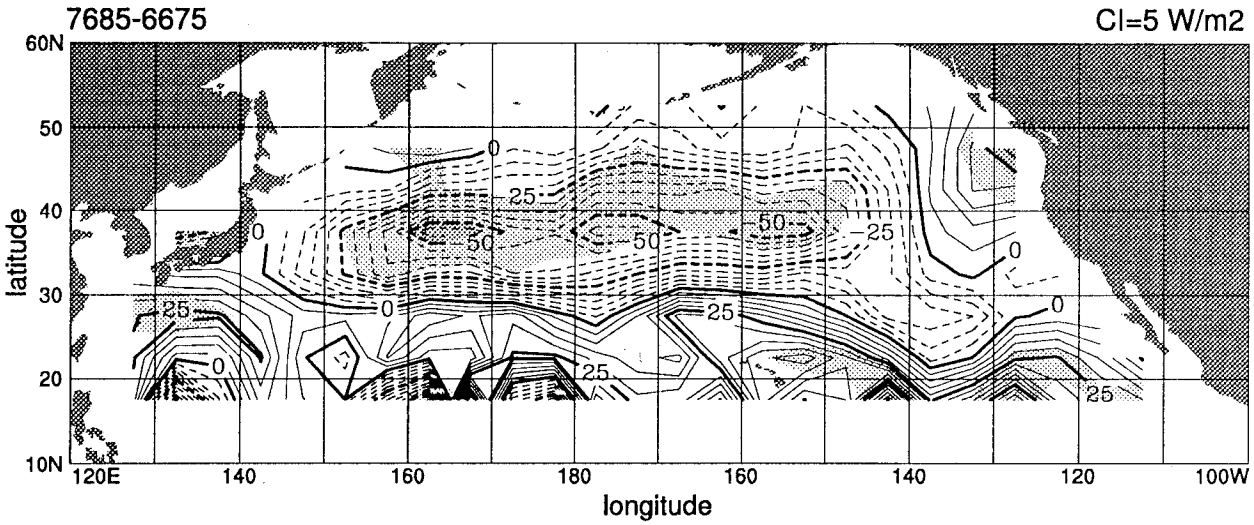

FIG. 8. As in Fig. 6 except for the wintertime heat divergence in the surface Ekman layer.

(warming) in the corresponding region (Fig. 2a). In order to solve this discrepancy, the changes in ocean circulation are considered in the next subsection.

c. Intensification of the subtropical gyre

The change in the Aleutian low due to the activity of the PNA pattern (Fig. 7) influences not only the strength of the Ekman heat transport but also the wind-driven ocean circulation. Figure 10 shows the time series of the annual mean Sverdrup transport at 30°N, 130°E, where the transport is largest in the subtropical gyre in the North Pacific. The transport rapidly increased in the mid-1970s. Furthermore, there is a larger transport during 1976–85 compared to 1966–75 throughout the whole area of the subtropical gyre (Fig. 11). Hence, it is suggested the subtropical gyre was spun up after the mid-1970s due to intensification of the Aleutian low and the associated westerlies.

In order to understand the oceanic manifestation of the gyre intensification, we present Kuroshio transports evaluated at two sections by Qiu and Joyce (1992) and Kawabe (1995). Qiu and Joyce (1992) calculated the Kuroshio transport along the 137°E section using hydrographic data from the Japan Meteorological Agency (JMA). Figure 12 displays time series of these transports from Table 2 of Qiu and Joyce (1992). The time mean transport during 1976–82, 53.9 Sv, is significantly larger than 42.9 Sv during 1969–75.

Figure 13 shows the temporal variability of the geo-

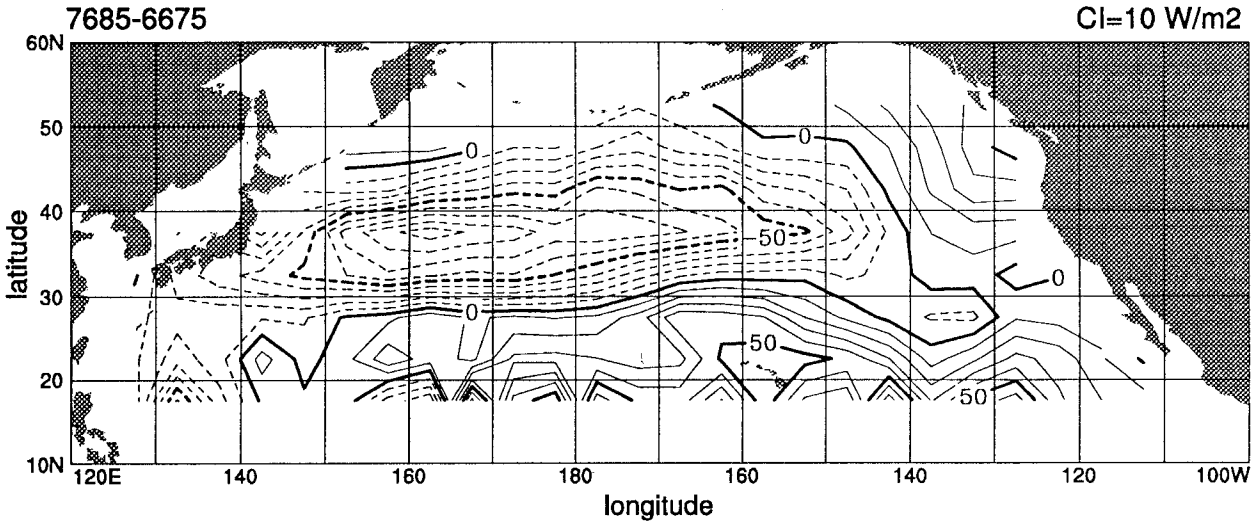

FIG. 9. Sum of the difference of the net heat flux through the surface (Fig. 6) and the difference of the Ekman heat divergence (Fig. 8). Contour intervals are 10 Wm^{-2}.

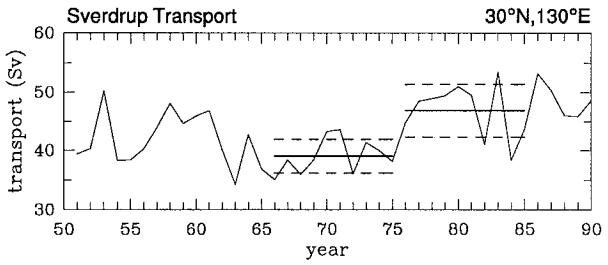

FIG. 10. Time series of the annual mean Sverdrup transport at 30°N, 130°E. Means and standard deviations for 1966–75 and 1976–85 are indicated.

strophic volume transport of the Kuroshio referred to 700 db, at the PN line in the East China Sea from Kawabe (1995). The transport was originally evaluated by the Nagasaki Marine Observatory of the JMA using two different methods, the one by Saiki (1982) and other from the *Oceanographic Prompt Reports* of that observatory. Comparing the transports computed using the two different methods, Kawabe (1995) added 2.2 Sv (Sv $\equiv 10^6$ m^3 s^{-1}) to the transports before 1972 estimated by using Saiki's method (for details, see his paper). It shows a transport of 25.6 Sv during 1976–85, which is also significantly larger than that during 1966–75 (22.5 Sv). The path of the Kuroshio south of Japan tended to be in a large meander phase after the mid-1970s. This may have a connection to the increased Kuroshio transport and the spinup of the subtropical gyre. Both of the above results indicate that the Kuroshio transport increased after the mid-1970s.

There is further evidence of gyre intensification. The meridional difference (29°N minus 39°N) of temperature averaged vertically from the surface to 400 m and zonally 150° to 160°E, which corresponds to the Kuroshio Extension area, is shown in Fig. 14. It increased continuously after the mid-1970s. Considering the thermal wind relation, this increasing baroclinicity reveals the subtropical gyre being spun up, which is concurrent with the intensification of the Sverdrup transport during 1976–85. Watanabe and Mizuno (1994) also demonstrated that the main thermocline was deeper after 1975 in the subtropical gyre.

The above results reveal that the subtropical gyre in the North Pacific strengthened after the mid-1970s. Although we are not able to evaluate the heat transport by the Kuroshio, it is plausible that the amount of warm water advected by the Kuroshio from lower latitudes to south of Japan became larger as a result of the spinup of the gyre. There is a similar difference in the heat flux in the western part of the subtropical gyre between the two decades as in the central North Pacific, but the increased advection of warm water prevented the temperature in the former area from becoming colder. Figure 15 shows a time series of net heat flux in the Kuroshio, the Kuroshio Extension, and the central North Pacific. In the central North Pacific, the rapid rise occurred in the mid-1970s. This abrupt change could have been caused by intensification of the westerlies over that area, because the sum of the sensible and latent heat fluxes is highly correlated with the wind speed over that area (Cayan 1992b). On the other hand, the heat flux increased gradually after the mid-1970s in the Kuroshio and the Kuroshio Extension areas. Because the correlation between the atmospheric PNA pattern and the wind speed is small over these areas (Cayan 1992b) and the Kuroshio transport increased after the mid-1970s, we can conclude that the gradual increase of heat release is a result of the increased advection of the warm water by the Kuroshio. This indicates that the warmer temperature in the southwestern part of the NPSTMW during 1976–85 arises from a combination of increased advection from lower latitudes and increased heat release to the atmosphere.

In summary, in the central North Pacific, where the westerlies strengthened after the mid-1970s, although surface heat release significantly increased, the heat loss due to the Ekman heat divergence was a significant factor in the decrease of the temperature of the NPCMW and the northeastern part of the NPSTMW. The change in ocean circulation forced by the intensification of the westerlies led to increased advection of warm water in the northwestern part of the subtropical gyre, which caused an increase in heat release to the atmosphere. Therefore, in spite of a larger amount of heat release, advection of warm water prevented the southeastern NPSTMW from becoming colder.

5. Concluding remarks

We have investigated temporal changes in the properties of NPSTMW and NPCMW that occurred around the mid-1970s, comparing data composited for the two decades bounded by the mid-1970s: 1966–75 and 1976–85. Properties of the two mode waters changed greatly after the mid-1970s. NPCMW was colder and more widely distributed during 1976–85. In the NPSTMW formation area, warmer water occupied the southwestern part, and colder water occupied the northeastern part during 1976–85.

In the central North Pacific, the decreased temperature of the mode waters was caused by the combined effect of increased heat release from the ocean to the atmosphere and increased heat divergence in the Ekman layer, with the latter component being dominant. The warming in the southwestern part of the NPSTMW area, however, could not be explained by the above mechanism alone. Since the Sverdrup transport of the subtropical gyre and the Kuroshio transport increased after the mid-1970s, it was suggested that the increased advection of warm water from lower latitudes to south of Japan by the Kuroshio was the major cause of the warming.

The long-term variability of the monthly SST tendency in winter is quite consistent with that of the heat

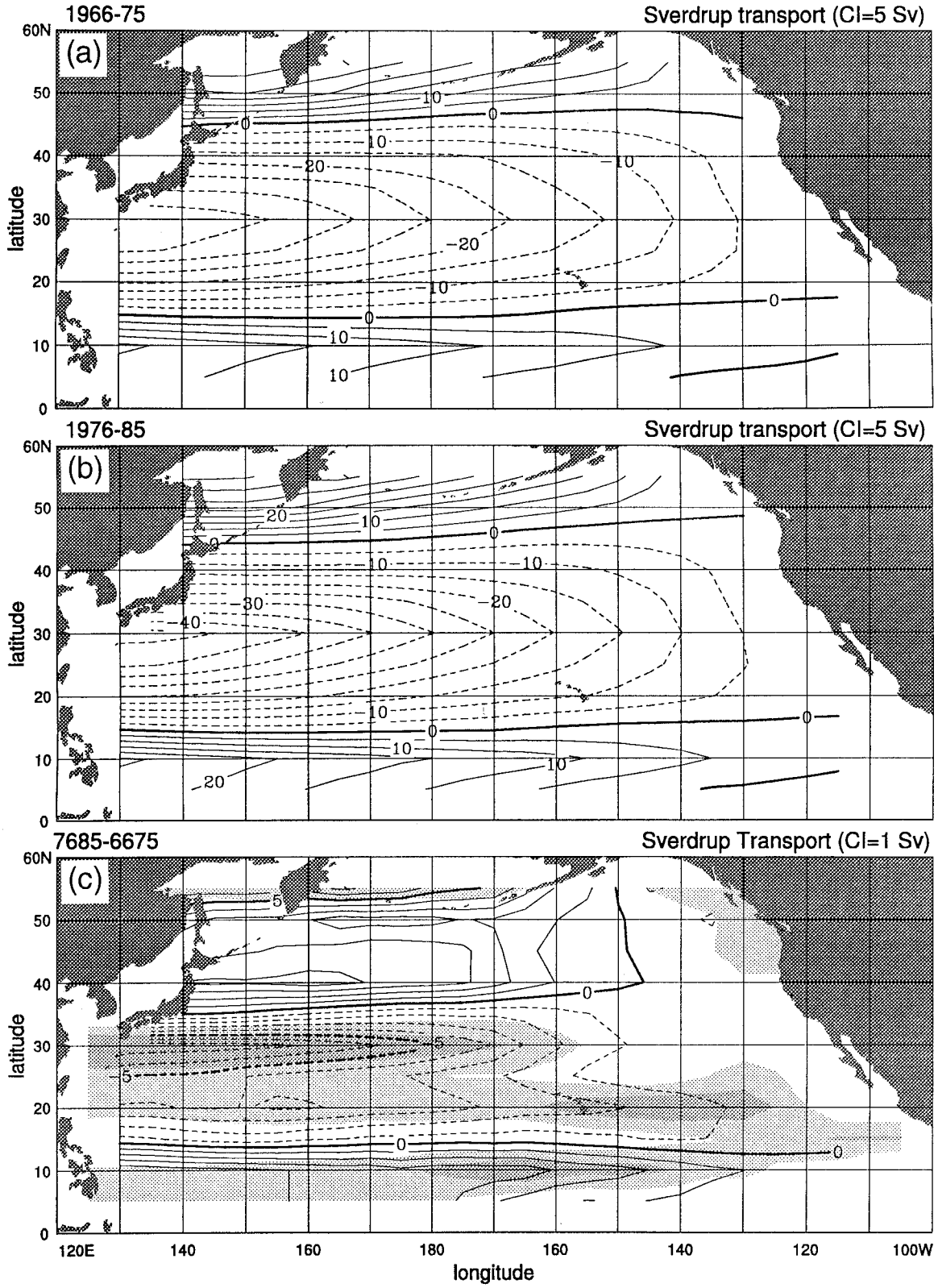

FIG. 11. Annual mean Sverdrup transport fields for (a) 1966–75, (b) 1976–85, and (c) the difference between two decades. Contour intervals are 5 Sv for (a) and (b), and 1 Sv for (c). Areas with confidence greater than 90% are hatched lightly and those with confidence greater than 99% darkly.

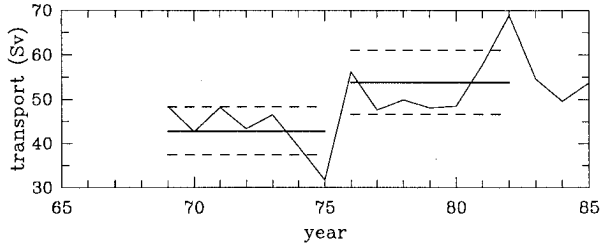

FIG. 12. Time series of the volume transport of the Kuroshio across the 137°E section evaluated by Qiu and Joyce (1992). Means and standard deviations for 1969–75 and 1976–82 are indicated.

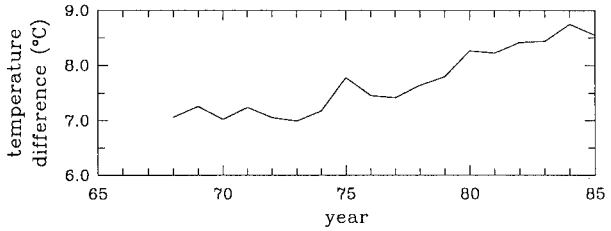

FIG. 14. Time series of the meridional difference of the annual mean temperature that is averaged vertically from 0 to 400 m and zonally from 150° to 160°E. The difference is taken for the value at 29° minus at 39°N and smoothed using a 3-yr running mean.

flux in winter (Cayan 1992c). Increased heat release to the atmosphere is related to the negative SST tendency. On the other hand, SST anomalies reflect atmosphere–ocean interaction in either direction. The area south of Japan is where increased advection from lower latitudes caused increased heat release to the atmosphere, and wintertime SST anomalies were not lower than those in the previous decade, even despite the negative SST tendency in winter.

Bingham et al. (1992) suggested the impact of gyre intensification on NPSTMW distribution. In their analysis, both the variations of NPSTMW on interannual and longer timescales are included, so they could not clearly distinguish NPSTMW variations characteristic of the two typical timescales. In this study, we chose two quasi-steady-state periods and averaged over a time span longer than the interannual timescale. We showed that the properties of the NPSTMW changed as a result of gyre spinup on the decadal timescale, which raised the temperature in the formation area.

The importance of geostrophic currents such as the Kuroshio was emphasized in this study. Since the long-term variations of the ocean circulation such as the spinup or spindown of the gyre vary the strength of the ocean currents in the northwestern part of the subtropical gyre, these influence the decadal variability of the upper thermal structure in that area. Furthermore, the properties and distribution of NPSTMW are directly affected by the spatial variations of the Kuroshio recirculation system, for example, variations in the behavior of eddies, the meander of the Kuroshio Extension (Suga and Hanawa 1995b), which may be related to decadal changes in ocean currents (Kawabe 1995). Hence, it is necessary to reproduce these behaviors in numerical models in order to simulate changes in NPSTMW and evaluate the role of heat transport by the Kuroshio on the decadal timescales.

SST anomalies in the NPCMW formation area have been investigated by many authors showing large variability on the decadal timescales. Temperature anomalies in NPCMW are advected by the gyre flow to lower latitudes on decadal timescales (Huang and Qiu 1994; Watanabe and Mizuno 1994). Although there is no clear

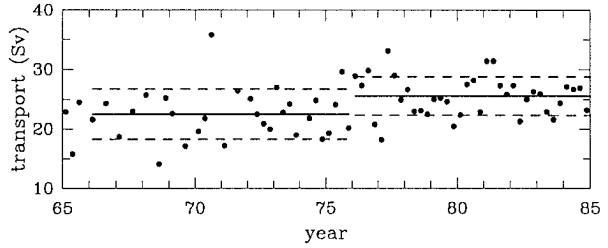

FIG. 13. Time series of the volume transport of the Kuroshio across the PN line evaluated by Kawabe (1995). This line runs approximately from 29°N, 126°E to 27°N, 128°E. Means and standard deviations for 1966–75 and 1976–85 are indicated.

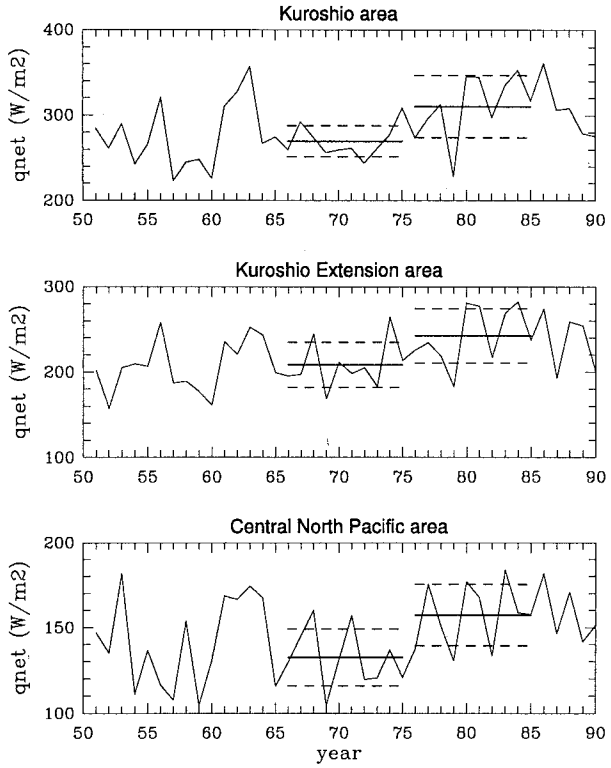

FIG. 15. Time series of wintertime net heat flux spatially averaged in the Kuroshio (30°–35°N, 130°–145°E), the Kuroshio Extension (30°–35°N, 145°–160°E), and the central North Pacific (35°–45°N, 170°E–170°W) areas. Means and standard deviations for 1966–75 and 1976–85 are indicated.

observational evidence that variations in tropical SST are affected by the midlatitude upper ocean, it is important to discern the temporal variability of NPCMW and its advection so that we may understand decadal climate variability.

Acknowledgments. We would like to thank Dr. Youichi Tanimoto for providing the wind stress, heat flux, and SST data used in this study. We would also like to thank Dr. Toshio Suga and other members of Physical Oceanography Group, Tohoku University, for many valuable discussions. Kuroshio transport data provided by Dr. Masaki Kawabe were useful. Dr. Frederick M. Bingham did careful and extensive English editing and gave useful comments. Comments and encouragement from anonymous reviewers and editor Dr. Dennis W. Moore were particularly helpful in improving this manuscript. This study was made as a part of ''Data Analysis of the Oceanic Variability of the Midlatitude North Pacific,'' which was financially supported by the Japan Marine Science and Technology Center, and as a part of the J-GOOS, which was financially supported by the Japanese Administration of Education, Science and Culture.

REFERENCES

Bingham, F. M., 1992: The formation and spreading of subtropical mode water in the North Pacific. *J. Geophys. Res.,* **97,** 11 177–11 189.

——, T. Suga, and K. Hanawa, 1992: Comparison of upper ocean thermal conditions on the western North Pacific between two pentads: 1938–42 and 1978–82. *J. Oceanogr.,* **48,** 405–425.

Cayan, D. R., 1992a: Variability of latent and sensible heat fluxes estimated using bulk formulae. *Atmos.–Oceans,* **30,** 1–42.

——, 1992b: Latent and sensible heat flux anomalies over the northern oceans: The connection to monthly atmospheric circulation. *J. Climate,* **5,** 354–369.

——, 1992c: Latent and sensible heat flux anomalies over the northern oceans: Driving the sea surface temperature. *J. Phys. Oceanogr.,* **22,** 859–881.

Davis, R. E., 1976: Predictability of sea surface temperature and sea level pressure anomalies over the North Pacific Ocean. *J. Phys. Oceanogr.,* **6,** 249–266.

Deser, C., and M. L. Blackmon, 1995: On the relationship between tropical and North Pacific sea surface temperature variations. *J. Climate,* **8,** 1677–1680.

Hanawa, K., 1987: Interannual variations in the winter-time outcrop area of Subtropical Mode Water in the western North Pacific Ocean. *Atmos.–Ocean,* **25,** 358–374.

——, and T. Suga, 1995: A review on the subtropical mode water in the North Pacific (NPSTMW). *Biogeochemical Process and Ocean Flux in the Western Pacific,* H. Sakai and Y. Nozaki, Eds., Terra Science, 613–627.

——, P. Rual, R. Bailey, A. Sy, and M. Szabados, 1995: A new depth-time equation for Sippican or TSK T-7, T-6 and T-4. *Deep-Sea Res.,* **42,** 1423–1451.

——, S. Ishizaki, and Y. Tanimoto, 1996: Strengthening of wintertime midlatitude westerlies over the North Pacific since mid 1970s. *J. Meteor. Soc. Japan,* **74,** 715–721.

Haney, R. L., 1980: A numerical case study of the development of large-scale thermal anomalies in the central North Pacific Ocean. *J. Phys. Oceanogr.,* **10,** 541–556.

——, 1985: Midlatitude sea surface temperature anomalies: A numerical hindcast. *J. Phys. Oceanogr.,* **15,** 787–799.

Huang, R. X., and B. Qiu, 1994: Three-dimensional structure of the wind-driven circulation in the subtropical North Pacific. *J. Phys. Oceanogr.,* **24,** 1608–1622.

Kawabe, M., 1995: Variations of current path, velocity, and volume transport of the Kuroshio in relation with the large meander. *J. Phys. Oceanogr.,* **25,** 3103–3117.

Levitus, S., 1982: *Climatological Atlas of the World Ocean.* NOAA Prof. Paper No. 13, U.S. Govt. Printing Office, 173 pp.

Masuzawa, J., 1969: Subtropical Mode Water. *Deep-Sea Res.,* **16,** 463–472.

——, 1972: Water characteristics of the North Pacific central region. *Kuroshio, It's Physical Aspects,* H. Stommel and K. Yoshida, Eds., Uniwersity of Tokyo Press, 95–127.

Miller, A. J., D. R. Cayan, T. P. Barnett, N. E. Graham, and J. M. Oberhuber, 1994: Interdecadal variability of the Pacific Ocean: Model response to observed heat flux and wind stress anomalies. *Climate Dyn.,* **9,** 287–302.

Nakamura, H., 1996: A pycnostad on the bottom of the ventilated portion in the central subtropical North Pacific: Its distribution and formation. *J. Oceanogr.,* **52,** 171–188.

National Oceanographic Data Center, 1991: Global ocean temperature and salinity profiles. National Oceanographic Data Center Informal Report No. 12, 20 pp.

Nitta, T., and S. Yamada, 1989: Recent warming of tropical sea surface temperature and its relationship to the Northern Hemisphere circulation. *J. Meteor. Soc. Japan,* **67,** 699–706.

Qiu, B., and T. M. Joyce, 1992: Interannual variability in the mid- and low-latitude western North Pacific. *J. Phys. Oceanogr.,* **22,** 1062–1079.

Saiki, M., 1982: Relation between the geostrophic flux of the Kuroshio in the Eastern China Sea and its large meanders in south of Japan. *Oceanogr. Mag.,* **32,** 11–18.

Suga, T., and K. Hanawa, 1990: The mixed-layer climatology in the northwestern part of the North Pacific subtropical gyre and the formation of the Subtropical Mode Water. *J. Mar. Res.,* **48,** 543–566.

——, and ——, 1995a: Interannual variations of North Pacific subtropical mode water in the 137°E section. *J. Phys. Oceanogr.,* **25,** 1012–1017.

——, and ——, 1995b: The subtropical mode water circulation in the North Pacific. *J. Phys. Oceanogr.,* **25,** 958–970.

——, ——, and Y. Toba, 1989: Subtropical Mode Water in the 137°E section. *J. Phys. Oceanogr.,* **19,** 1605–1618.

——, Y. Takei, and K. Hanawa, 1997: Thermostad distribution in the North Pacific subtropical gyre: The central mode water and the subtropical mode water. *J. Phys. Oceanogr.,* **27,** 140–152.

Tanimoto, Y., N. Iwasaka, and K. Hanawa, 1993: Characteristic variations of sea surface temperature with multiple time scales on the North Pacific. *J. Climate,* **6,** 1153–1160.

——, ——, ——, and Y. Toba, 1997: Relationships between sea surface temperature, the atmospheric circulation and air–sea fluxes on multiple time scales. *J. Meteor. Soc. Japan,* in press.

Tokioka, T., A. Kitoh, and S. Nakagawa, 1992: Interaction between lower atmosphere and the ocean realized in a coupled atmosphere–ocean general circulation model. *Abstracts, Int. WCRP Symp.—Clouds and Ocean in Climate,* Nagoya, Japan, World Meteor. Org., 1.5–1.8.

Trenberth, K. E., 1990: Recent observed interdecadal climate changes in the Northern Hemisphere. *Bull. Amer. Meteor. Soc.,* **71,** 988–993.

——, and J. W. Hurrell, 1994: Decadal atmosphere–ocean variations in the Pacific. *Climate Dyn.,* **9,** 303–319.

Wallace, J. M., C. Smith, and Q. Jiang, 1990: Spatial patterns of atmosphere–ocean interaction in the northern winter. *J. Climate,* **3,** 990–998.

Watanabe, T., and K. Mizuno, 1994: Decadal changes of the thermal structure in the North Pacific. *Int. WOCE Newslett.,* **15,** 10–13.

Weare, B. C., 1989: Uncertainties in estimates of surface heat fluxes derived from marine reports over the tropical and subtropical oceans. *Tellus,* **41A,** 357–370.